DESI GFA Zeropoints and Throughput Validation

Aaron Meisner

1 GFA Throughput Prediction

In order to validate the system throughput as measured by the DESI GFA cameras, we must first perform an analysis to determine the expected throughput and photometric zeropoint. The primary goal of this analysis is to predict the r band AB magnitude of a source that would correspond to a total detected DESI GFA signal of 1 electron per second. The factors that contribute to determining the DESI GFA throughput are: the atmosphere, the Mayall telescope primary mirror reflectivity, the corrector throughput (including vignetting at the radius of the GFA cameras), the GFA r band filter transmission profile and the GFA detector quantum efficiency (QE). These individual factors are overplotted together in Figure 1.

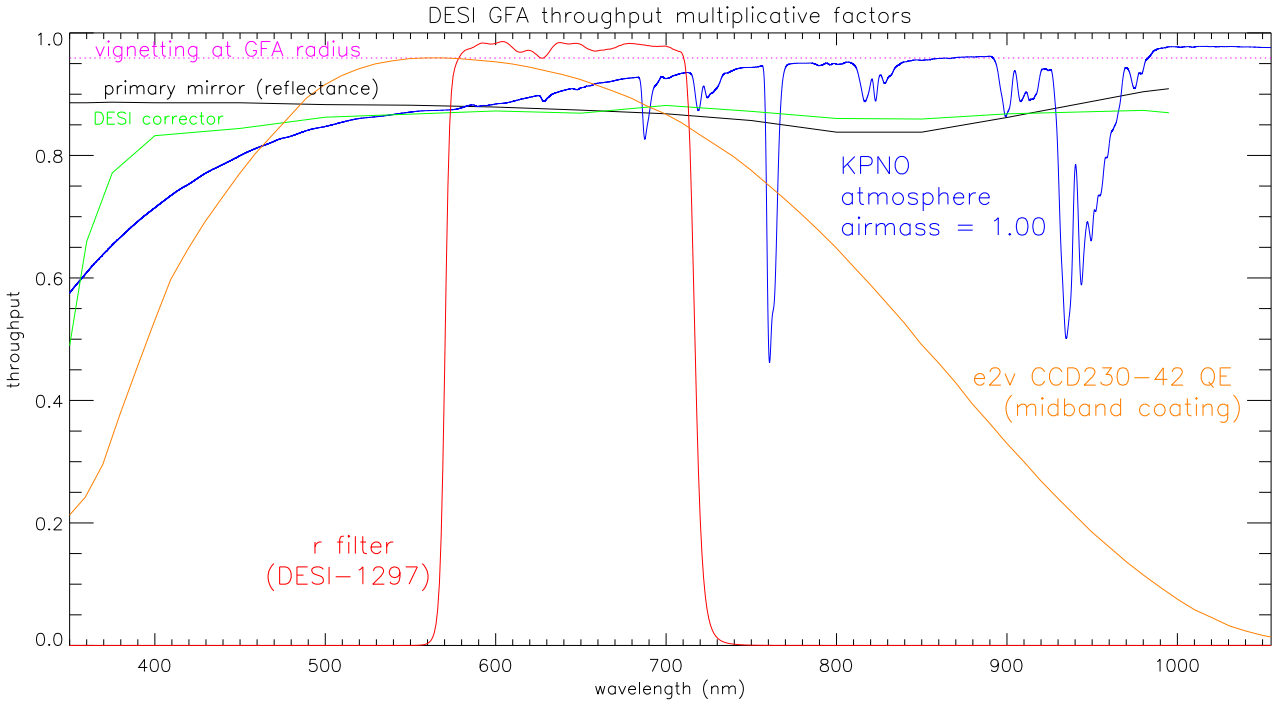

Figure 1: Summary of the multiplicative factors that contribute to determining the total DESI GFA throughput as a function of wavelength.

The atmospheric transmission is taken from a file called `ZenithExtinction-KPNO.fits`, found in the desimodel product[1]. The Mayall telescope primary mirror reflectivity, corrector throughput and vignetting were taken from DESI-347-v14 "Throughput Noise SNR Calcs". We adopt 1.574° for the radius of the GFA cameras based on template WCS solutions trained on Gaia star locations in real GFA images. The GFA filter transmission was extracted from DESI-1297 "GFA Filter verification data". The GFA CCD QE was extracted from the e2v data sheet "CCD230-42 Back Illuminated Scientific CCD Sensor", specifically the plot on page 4. Note that the DESI GFA detectors have the 'Basic midband coating' option (i.e., the green line in the data sheet's QE plot). The resulting total throughput is shown in Figure 2.

In order to use the total throughput curve to calculate a predicted zeropoint in AB magnitudes, we additionally need to take into account the mirror area. We adopt a value of 8.66 square meters for the Mayall primary mirror area based on DESI-347-v15. Combining the throughput curve, the definition of the AB magnitude system, and the

[1] `https://desi.lbl.gov/svn/code/desimodel/trunk/data/inputs/throughput/ZenithExtinction-KPNO.fits`

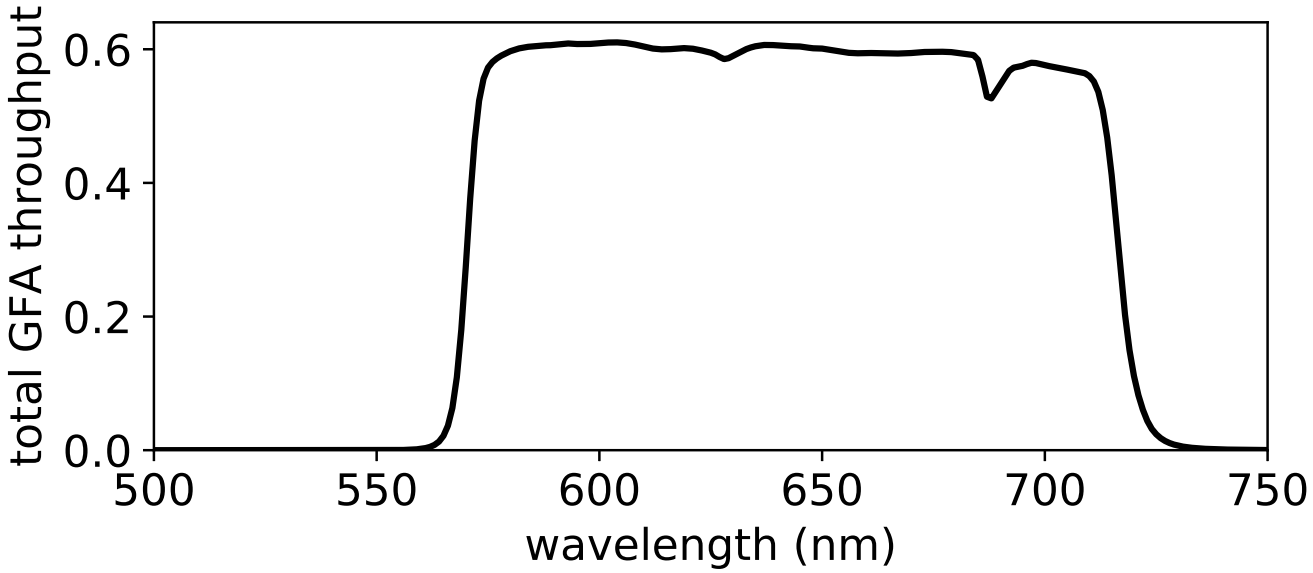

Figure 2: Total GFA throughput as a function of wavelength. The data shown in this figure have been uploaded as a supplementary file.

Mayall primary mirror area we calculate a predicted GFA zeropoint of $r = 27.026$ AB for a source with total detected signal of 1 electron per second (assuming airmass = 1). This computation is run using the following command:

```
calc_ci_zeropoint, /gfa
```

Where the `calc_ci_zeropoint.pro` code can be found in my `ci_throughput` GitHub repository[2].

2 GFA Gain

Before we can compare on-sky GFA measurements to our predicted zeropoint, we need to have accurate knowledge of how to convert from ADU (units of the raw GFA data) to electrons. Lab-measured GFA gains are available in a series of DESI DocDB entries (see Table 1), and a set of Mayall dome screen data were also taken on 20191027 specifically to enable post-installation gain measurements. My gain measurements based on the post-installation dome screen data are documented on the DESI wiki[3]. The lab gain measurements and my dome screen gain measurements are listed in Table 1.

My gain measurements based on the 20191027 dome screen data are in very good agreement with those based on the lab data, although the former are ∼0.9% higher than the corresponding lab gain measurements in the median. David Kirkby has also analyzed the same 20191027 dome screen data and was able to obtain even better agreement with the lab gain measurements (DESI-5315). We therefore adopt the lab gain measurements compiled from the various GFA acceptance reports when comparing our predicted zeropoint to the on-sky measurements. It seems clear that we should not expect our knowledge of the GFA gains to be a significant limitation in the comparison between measured and predicted zeropoints.

3 Input GFA On-sky Data

For this throughput study, we use a set of 22 GFA exposures taken on 20191025. The exposures have $21338 \leq$ EXPID ≤ 21360, with EXPID = 21350 omitted because of its short 1 second exposure time. The program name

[2] `https://github.com/ameisner/ci_throughput`

[3] `https://desi.lbl.gov/trac/wiki/Commissioning/Planning/gfachar/gain_20191027`

(PROGRAM keyword header parameter) of this set of exposures is "dense fields". These exposures are all centered in the vicinity of (RA, Dec) = (80°, 30°), which is near the Galactic anticenter at (l_{gal}, b_{gal}) ≈ (176, −4). These exposures were chosen for the following reasons:

- They were taken during a photometric time period.
- They were taken in reasonably good seeing. The median FWHM is 0.98″ (min = 0.94″, max = 1.49″, dispersion = 0.12″).
- They are taken in a region of high source density. This provides more sources per exposure to compare against PS1, better assurance of successful astrometric calibration, and also enables high-quality PSF modeling.
- They are relatively long GFA exposures (the unique exposure times are 30 seconds and 60 seconds), further improving the density of well-detected sources.
- The airmass is very nearly 1, minimizing the impact of any inaccuracies in the atmospheric transmission component of GFA throughput prediction.
- All six cameras worth of guide GFA images are available for all exposures in this sequence.
- The exposures were dithered at a scale of ∼30″ per coordinate, so that we are not always sampling the same stars at the same GFA pixel locations during every single exposure.

In this study we only consider the six in-focus guide cameras, and ignore the four out of focus GFA cameras.

4 Source Catalogs

Source detection and astrometric calibration were performed with the `gfa_reduce` GFA off-line reduction package for each guide camera of each GFA exposure discussed in §3. Astrometric calibration is necessary in order to identify the correct PS1 match to each GFA detection (§5). Astrometric calibration was successful for all cameras of all exposures. For this study, we perform aperture photometry in a 5 pixel radius circular (in pixel space) aperture. We then correct this aperture photometry to be as close as possible to "total light". This is accomplished by first building a PSF model for each guide camera of each GFA exposure, then using this PSF model to compute an aperture correction from flux within the 5 pixel radius aperture to total light within the full extent of the PSF model, and finally multiplying the aperture photometry by this aperture correction factor. Each PSF model is 61 pixels on a side. The fluxes are measured in raw ADU so as to avoid baking in a specific flat field correction, given that different pipelines may use different flat field corrections and/or the master flat could evolve over time as more calibration data are obtained.

The per-exposure catalogs have been concatenated and uploaded as a supplementary file[4]. The aperture fluxes in raw ADU are in the column named COUNTS_PER_SECOND and the aperture correction factor is in a column named APCORR_FAC.

5 PS1 Photometry Comparison

The sky location of the data set used in this study is outside of the DESI pre-imaging footprint, but does have Pan-STARRS r band data available. We match to PS1 using a radius of 1″. The row-matched table of PS1 counterparts is also uploaded as a supplementary file[5]. We define a GFA instrumental r band magnitude as:

$$r_{inst} = -2.5 \times \log_{10}(\text{COUNTS\_PER\_SECOND} \times \text{APCORR\_FAC}) \quad (1)$$

The zeropoint is then simply the difference between r_{ps1} and r_{inst}.

Since the sky location being considered is in the Galactic plane and the comparison sources being used are not especially faint (see scatter plots in Appendix B), we assume that all matched sources are pointlike stars rather than extended galaxies. The version of the PS1 catalog being used ('fitscat_qz_trim') was also constructed with a

[4] row_matched_dense_fields-gfa.all_cameras.fits
[5] row_matched_dense_fields-ps1.all_cameras.fits

star-galaxy separation cut meant to retain only stars, further indicating the lack of a need for attempting to make source morphology corrections.

The scatter plots of instrumental versus PS1 mags in Appendix B show that, over the range of magnitudes used to fit the zeropoint (rightward of vertical yellow lines), the model of $r_{inst} = r_{ps1} - zp$, with zp being a scalar offset per-camera per-amp fits very well. This model is shown as the red line with slope of 1 in each Appendix B scatter plot.

6 Measured Zeropoint Values

Table 2 lists the zeropoint values obtained in terms of both ADU/s and e-/s on a per-amp basis for all six guide GFA cameras. The values quoted in Table 2 for each (camera, amp) pair are obtained by taking the median of the per-exposure zeropoint values derived for that (camera, amp) pair. The zeropoints in terms of ADU are applicable to the raw data — they do not have any flat fielding baked in. In all cases the zeropoints are meant to correspond to total light rather than signal within some nominal aperture. The median zeropoint in terms of e-/second is $r = 27.062$ AB. This is slightly (3.4%) deeper than the predicted zeropoint (§1) of $r = 27.026$ AB for a source with total detected signal of 1 e-/second.

6.1 Confirming That ADU Zeropoints Track Gain as Expected

Amp pairs E/F and G/H should be at approximately the same radial distance from the focal plane center for all cameras. Assuming for each camera that within each of these amp pairs the average vignetting, QE and filter transmission are all the same, then the difference in zeropoint for a 1 ADU source should track the difference in gain, with larger gain corresponding to a lower (brighter) ADU zeropoint magnitude. Based on these assumptions and the measured gains, we can predict the difference in zeropoints for amp pairs E/F and G/H and check whether this correlates with the measured differences in ADU zeropoints. The scatter plots in Figures 3 and 4 summarize this analysis, with one plot for the E/F amp pair and one plot for the G/H amp pair. Each data point in each plot represents one guide GFA camera. The plots show that the measured ADU zeropoints do track fairly well with expectations based on the gain differences. The lab-measured GFA acceptance report gains were used in making these plots.

A Confirming GFA EXPTIME

A key assumption underlying our comparison of the measured GFA zeropoints to our zeropoint prediction is that we are using the correct GFA exposure time in computing the signal as a rate in detected electrons per second. GFA exposure times in seconds are accessed via the EXPTIME header keyword. Given the discussion about GFA timestamp oddities (e.g., [desi-commiss 2976]) and the unshuttered cameras, I decided to check how well the integration time agrees with the reported EXPTIME. It's also particularly interesting to double check EXPTIME because there are relatively few ways that the measured GFA zeropoint could be slightly *deeper* than the prediction (as we have found, by ∼3-4%), but one such possibility is that the true GFA integration time is longer than what we are assuming based on the reported GFA EXPTIME values.

To address this, I measured the length of star trails in the 5 second untracked exposure EXPID = 24467 at zenith. I find an average trail length in GUIDE2 and GUIDE7 of 62.4 asec. For comparison, the length of the sidereal day and Dec give me a prediction of 63.8 asec trails during 5 seconds. So the prediction is 2.3% larger than the measurement. This could certainly be within the error margin of my measurement, but the agreement would be better if I assumed that EXPTIME is equal to the integration time plus the ∼100 ms time to shift the active image area's charge rather than simply the integration time (0.1 s / 5 s = 2%). Regardless, this seems like quite good agreement, and any issue at the ∼100 ms level would result in a negligible change to my derived zeropoints, which are based on images with relatively long 30-60 second exposure times.

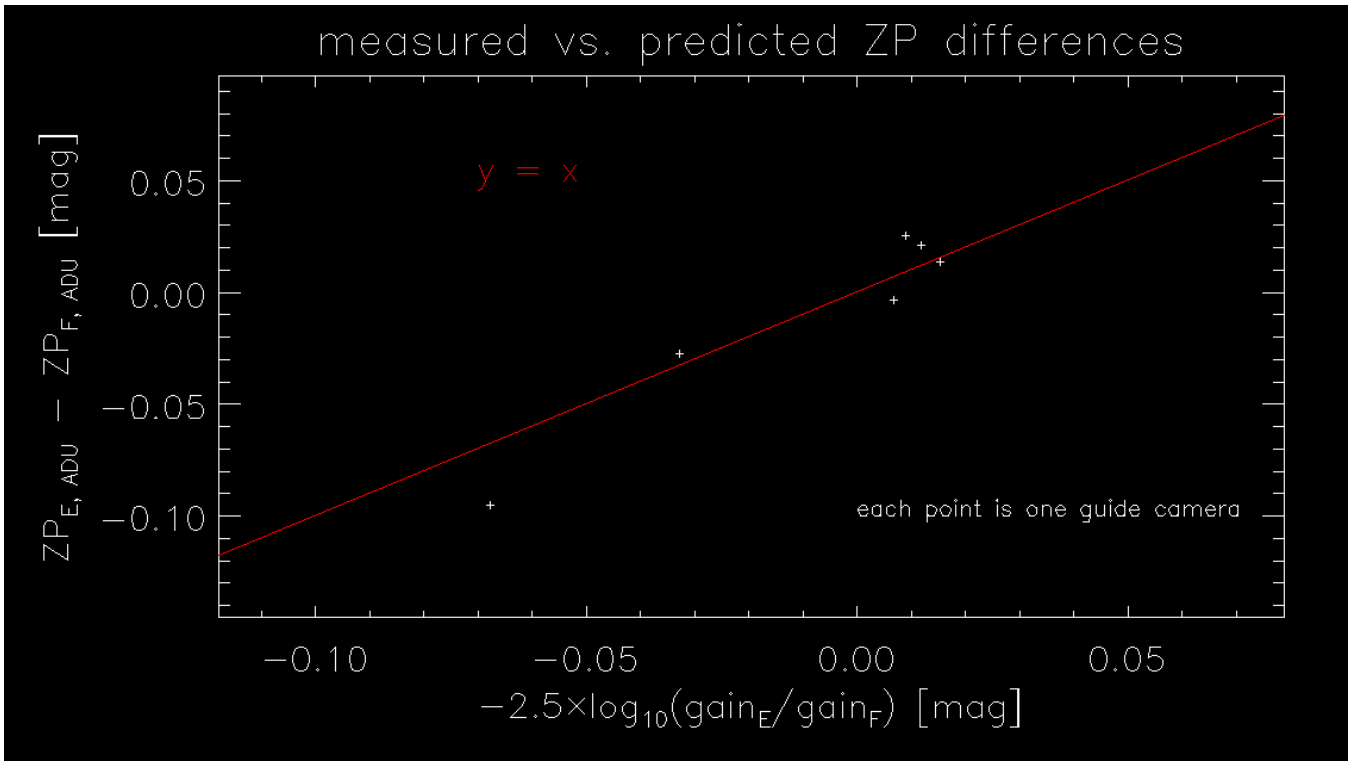

Figure 3: If we assume that the vignetting, QE, and filter transmission are the same for amps E and F within each guide camera, then the difference between the measured ADU zeropoints for these two amps within each guide camera should simply trace the difference in their gains. Based on these assumptions and the the known ratio of gains in amps E and F, we can make a per-camera prediction of the difference in ADU zeropoints between amp E and amp F. This predicted ADU zeropoint difference is the horizontal axis in this plot. The measured difference in ADU zeropoints between amps E and F is then plotted on the vertical axis. Each white plus mark represents a single guide GFA camera. The red line is y = x, not a fit. For this exercise, we again use the lab-measured acceptance GFA gains. The measured zeropoint differences between amps E and F do indeed trace the line y = x well — the measured ADU zeropoints pass this sanity check.

B Per-camera, Per-amp Photometry Scatter Plots

Appended below is the full set of per-exposure, per-camera, per-amp scatter plots of GFA instrumental magnitudes versus PS1 r band AB magnitudes for the set of exposures used during this study. The vertical yellow line indicates the magnitude threshold fainter than which GFA photometry was considered safe from potential saturation/nonlinearity. In each case the red line is fixed to have a slope of unity (the slope is not fit as a free parameter), and its y axis offset is the median of the difference between the GFA instrumental magnitudes and the PS1 AB magnitudes for (sufficiently faint) matched sources.

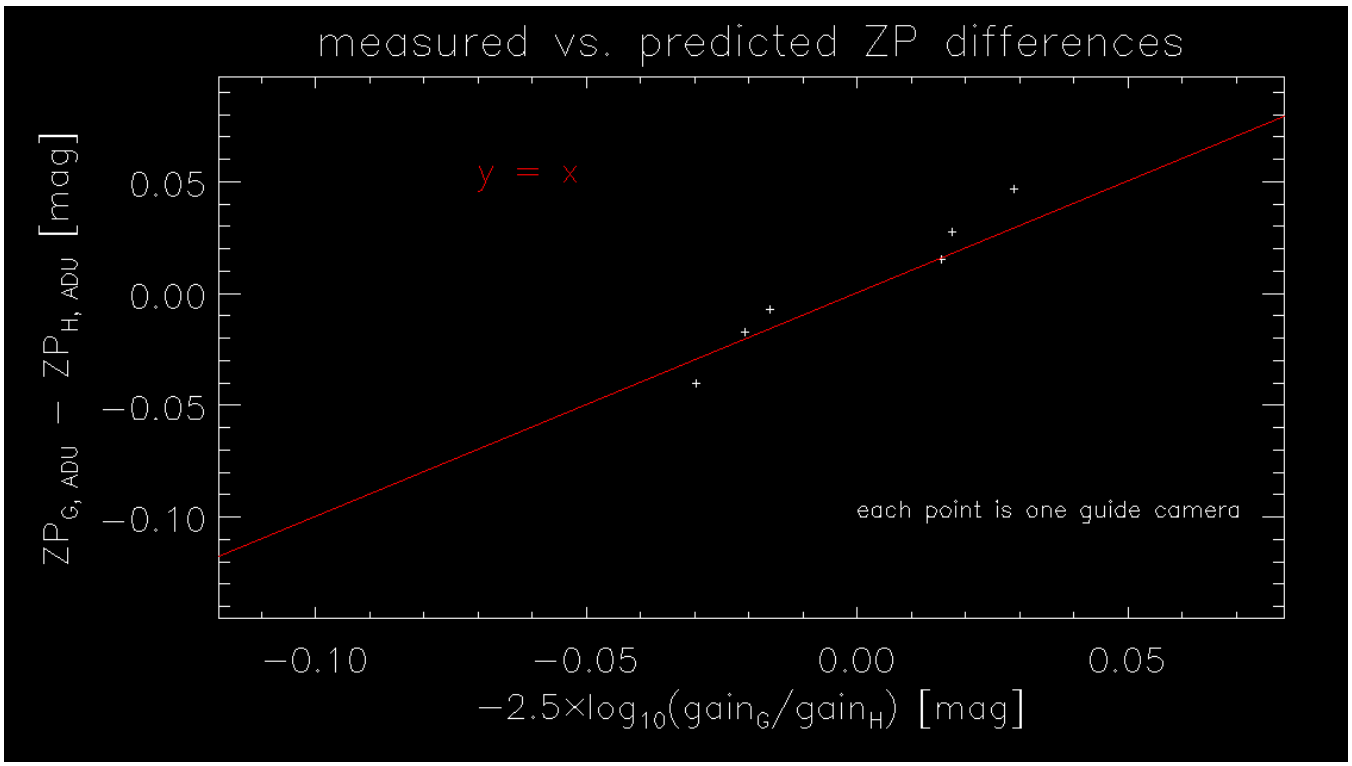

Figure 4: Same as Figure 3, but for amps G and H.

EXTNAME	GFA device	amp	20191027 gain (e-/ADU)	acceptance gain (e-/ADU)	acceptance ref.	region
GUIDE0	10	E	3.516	3.516	DESI-4750-v1	all
GUIDE0	10	F	3.575	3.545	DESI-4750-v1	all
GUIDE0	10	G	3.714	3.673	DESI-4750-v1	all
GUIDE0	10	H	3.581	3.574	DESI-4750-v1	all
FOCUS1	5	E	3.589	3.559	DESI-4675-v1	outer
FOCUS1	5	F	3.790	3.712	DESI-4675-v1	outer
FOCUS1	5	G	3.686	3.644	DESI-4675-v1	outer
FOCUS1	5	H	3.867	3.795	DESI-4675-v1	outer
GUIDE2	6	E	3.686	3.668	DESI-4680-v1	all
GUIDE2	6	F	3.763	3.708	DESI-4680-v1	all
GUIDE2	6	G	3.716	3.673	DESI-4680-v1	all
GUIDE2	6	H	3.788	3.733	DESI-4680-v1	all
GUIDE3	2	E	3.687	3.669	DESI-4665-v1	all
GUIDE3	2	F	3.624	3.560	DESI-4665-v1	all
GUIDE3	2	G	3.852	3.785	DESI-4665-v1	all
GUIDE3	2	H	3.785	3.729	DESI-4665-v1	all
FOCUS4	7	E	3.766	3.798	DESI-4713-v1	outer
FOCUS4	7	F	3.824	3.761	DESI-4713-v1	outer
FOCUS4	7	G	3.765	3.731	DESI-4713-v1	outer
FOCUS4	7	H	3.817	3.747	DESI-4713-v1	outer
GUIDE5	8	E	3.715	3.718	DESI-4716-v1	all
GUIDE5	8	F	3.792	3.741	DESI-4716-v1	all
GUIDE5	8	G	3.761	3.733	DESI-4716-v1	all
GUIDE5	8	H	3.779	3.787	DESI-4716-v1	all
FOCUS6	13	E	3.744	3.740	DESI-4908-v1	outer
FOCUS6	13	F	3.715	3.670	DESI-4908-v1	outer
FOCUS6	13	G	3.720	3.698	DESI-4908-v1	outer
FOCUS6	13	H	3.749	3.732	DESI-4908-v1	outer
GUIDE7	1	E	3.814	3.863	DESI-4662-v1	all
GUIDE7	1	F	3.606	3.629	DESI-4662-v1	all
GUIDE7	1	G	3.987	4.043	DESI-4662-v1	all
GUIDE7	1	H	3.906	3.967	DESI-4662-v1	all
GUIDE8	4	E	3.792	3.740	DESI-4672-v1	all
GUIDE8	4	F	3.855	3.793	DESI-4672-v1	all
GUIDE8	4	G	3.610	3.601	DESI-4672-v1	all
GUIDE8	4	H	3.728	3.698	DESI-4672-v1	all
FOCUS9	3	E	3.641	3.586	DESI-4747-v2	outer
FOCUS9	3	F	3.659	3.612	DESI-4747-v2	outer
FOCUS9	3	G	3.823	3.763	DESI-4747-v2	outer
FOCUS9	3	H	3.639	3.659	DESI-4747-v2	outer

Table 1: Comparison of gain measurements from pre-installation lab data taken as part of the GFA acceptance process (R. Casas) and post-installation dome screen data taken on 20191027. The final column lists the region of each amplifier used for my 20191027 gain measurement. All of each amplifier is used for the guide cameras, but for the focus cameras only the 'outer' half of each amp is used, in order to avoid the shaded area near the camera center.

camera	amp	ZP (total raw ADU/s)	ZP (total e-/s)	assumed gain (e-/ADU, from acceptance report)
GUIDE0	E	25.714	27.079	3.516
GUIDE0	F	25.689	27.063	3.545
GUIDE0	G	25.654	27.067	3.673
GUIDE0	H	25.695	27.078	3.574
GUIDE2	E	25.633	27.045	3.668
GUIDE2	F	25.612	27.035	3.708
GUIDE2	G	25.654	27.067	3.673
GUIDE2	H	25.627	27.057	3.733
GUIDE3	E	25.652	27.063	3.669
GUIDE3	F	25.679	27.058	3.560
GUIDE3	G	25.615	27.061	3.785
GUIDE3	H	25.623	27.052	3.729
GUIDE5	E	25.626	27.052	3.718
GUIDE5	F	25.630	27.062	3.741
GUIDE5	G	25.636	27.066	3.733
GUIDE5	H	25.621	27.066	3.787
GUIDE7	E	25.569	27.036	3.863
GUIDE7	F	25.664	27.063	3.629
GUIDE7	G	25.494	27.011	4.043
GUIDE7	H	25.512	27.008	3.967
GUIDE8	E	25.615	27.047	3.740
GUIDE8	F	25.601	27.048	3.793
GUIDE8	G	25.699	27.090	3.601
GUIDE8	H	25.652	27.072	3.698

Table 2: Summary of measured GFA zeropoints in terms of both ADU/s and e-/s, the latter adopting the lab-measured gains in converting from raw ADU to electrons.